EPJ Web of Conferences **137**, 08009 (2017) DOI: 10.1051/epjconf/201713708009
XIIth Quark Confinement & the Hadron Spectrum

Measurement of the WZ boson pair production cross section at 13 TeV and confidence intervals on anomalous triple gauge couplings with the ATLAS detector

Dimitrios Iliadis[1,2,a]
On behalf of the ATLAS collaboration

[1] *Aristotle University of Thessaloniki (AUTh)*
[2] *Laboratoire d'Annecy-le-Vieux de Particules de Physique (LAPP)*

Abstract. The WZ boson pair production at 13 TeV is measured using the ATLAS detector. Leptonic decays of the W and Z bosons to electrons and muons are considered using 2015 and 2016 data that correspond to a total integrated luminosity of 13.3 fb^{-1}. The differential cross-section as a function of jet multiplicity is also measured along with the charge-dependent W^+Z and W^-Z cross-sections and their ratio. Also, the integrated fiducial cross-sections ratio, measured at center-of-mass energies of 8 TeV and 13 TeV, is calculated. Finally, limits on anomalous triple gauge couplings are derived.

1 Introduction

The diboson production provides an important test of perturbative quantum chromodynamics (pQCD), especially now that next-to-next-to-leading-order (NNLO) calculations [12] become available. Deviations from the predictions of the Standard Model (SM) on diboson production cross-section may be a strong indication of new physics and are an excellent probe of the electroweak sector of the SM. New physics could manifest itself as a modification of the triple and quartic gauge couplings (aTGC, aQGC respectively) and consequently, as an enhancement in the production cross-section. Among the diboson processes, the WZ has a larger cross-section than the ZZ and a cleaner experimental signature than the WW process.

This article presents the measurements of the $W^{\pm}Z$ production cross-section in pp collisions at a centre-of-mass energy of $\sqrt{s}$=13 TeV. The data were collected in 2015 and 2016 by the ATLAS [1] experiment at the LHC and the results presented here correspond to a total integrated luminosity of 13.3 fb^{-1}, obtained in 2015 (3.2 fb^{-1}, [3]) and 2016 (10.1 fb^{-1}, [4]). The inclusive production cross-sections in the fiducial and the total phase-spaces, as well as the ratio of the cross-sections at 13 TeV and 8 TeV and the W^+Z/W^-Z cross-section ratio are shown here. The differential cross-sections, as a function of the jet multiplicity, the Z-boson p_T and the transverse mass of the W-boson are also presented. Finally, confidence intervals are derived for anomalous triple gauge couplings from the transverse mass spectrum of the $W^{\pm}Z$ system.

[a] e-mail: Dimitrios.Iliadis@cern.ch

2 Experimental signatures, fiducial phase-space and background estimation

The WZ experimental signature consists of three high-p_T, isolated leptons accompanied by missing transverse energy, E_T^{miss}. The invariant mass of two same-flavour, opposite-charge leptons must be constistent with the mass of the Z-boson while the transverse mass of the system of the third lepton and the E_T^{miss} must be consistent with the mass of the W-boson. Only decays of the bosons to electrons and muons are considered, leading to four distinct final-states: eee, $e\mu\mu$, μee and $\mu\mu\mu$.

2.1 Fiducial phase-space

The fiducial phase-space (PS) definition was kept identical to the 8 TeV WZ publication [2] in order to be able to calculate the integrated cross-section ratio at the two centre-of-mass energies. A user-defined algorithm to compute the detector acceptance was developed (namely the "Resonant Shapes" algorithm [2]). The algorithm associates the generator-level leptons to their mother bosons. Table 1 lists the selection criteria used in the fiducial PS. The total PS is defined by the sole requirement: 66 GeV $< m_Z <$ 116 GeV.

Table 1. Selection criteria for the definition of the fiducial PS [4].

Fiducial Phase-Space
$\lvert m_{\ell\ell} - m_Z \rvert < 10$ GeV
$m_T^W > 30$ GeV
Z leptons: $p_T > 15$ GeV
W leptons: $p_T > 20$ GeV
$\lvert\eta_\ell\rvert < 2.5$ for all three leptons
$\Delta R(\ell, \ell) > 0.3$ between W and Z leptons
$\Delta R(\ell, \ell) > 0.2$ between Z leptons

2.2 Background processes

The background processes that mimic the WZ experimental signature can be divided into two categories: the irreducible and the reducible sources.

2.2.1 Irreducible background

Processes belonging to this category are ZZ, $VVV, (V : W, Z)$, tZ and $t\bar{t}V$. These have at least three prompt[1] leptons in their final state with the fourth escaping detection (either because it is falling outside the detector acceptance or because it fails identification). This background category is estimated using the Monte Carlo (MC) samples.

2.2.2 Reducible background

This second category consists of the $V + jets$, $V + \gamma, (V : W, Z)$, $t\bar{t}$ and WW processes where at least one of the final-state leptons is characterised as "fake", i.e. coming from heavy flavour decays or from a jet misidentified as a lepton or from a photon conversion (in the case of an electron). It is estimated using a data-driven method (namely the matrix method [5]).

[1] Prompt leptons are defined as originating from the decays of the vector bosons.

3 Yields, control distributions and systematic uncertainties

Figure 1 shows the distributions of the Z-boson invariant mass and p_T, where the Powheg+Pythia MC prediction is used for the SM signal contribution. The simulated $W^{\pm}Z$ events and the leptonic decays of the vector bosons are generated at NLO using the Powheg-box v2 [6] MC generator, interfaced to pythia 8.210 [7] parton shower model using the AZNLO [8] set of tuned parameters. Table 2 summarises the predicted and observed number of events along with the estimated contribution from various background sources; only statistical uncertainties are shown. In Table 3 a summary of the systematic uncertainties is given. These include uncertainties in the correction procedure in MC for detector effects (i.e finite resolution, imperfect efficiency), theoretical uncertainties and uncertainties related to luminosity as well as the background estimation method.

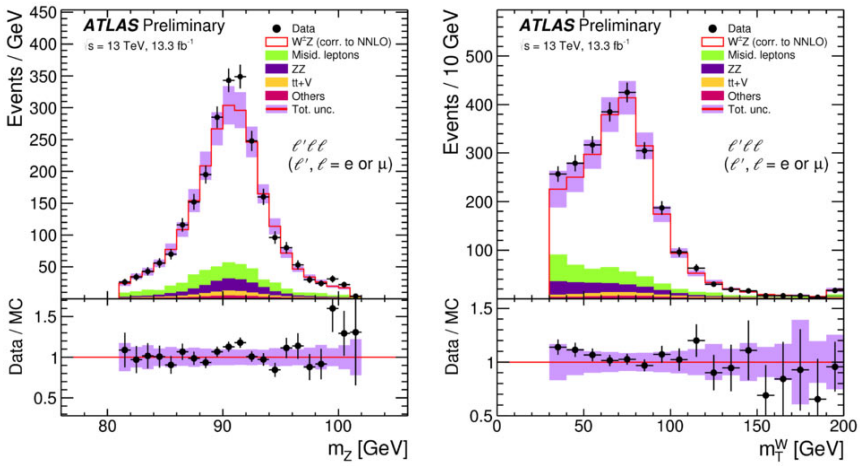

Figure 1. Reconstructed Z-boson mass m_Z and transverse mass of the W-boson, m_T^W. The points correspond to the data, and the histograms correspond to the predictions of the different SM processes. The sum of the background processes with fake or non-prompt leptons is labelled “Misid. leptons". The shaded violet band is the total uncertainty on this prediction [4].

4 Results

The measured fiducial cross-sections in the four channels are combined using a χ^2 minimisation method [9–11]. The results presented in the following represent the first two measurements in the new energy regime of 13 TeV. They correspond to the 2015 dataset with 3.2 fb^{-1} and to the 2016 dataset with 10.1 fb^{-1}, giving a total integrated luminosity of 13.3 fb^{-1}. Unless otherwise stated, the results shown will be the ones obtained with the total integrated luminosity of 13.3 fb^{-1}.

4.1 Integrated cross-sections

Figure 2 shows the ratio of the measured fiducial cross-sections per channel over the theoretical predictions using Powheg+Pythia at NLO QCD. The combined measured fiducial cross-section is:

$$\sigma^{fid.}_{W^{\pm}Z\to\ell'\nu\ell\ell} = 66.2 \pm 1.8(stat.) \pm 3.6(sys.) \pm 2.1(lumi.) fb. \quad (1)$$

Table 2. Observed and expected number of events after the WZ inclusive selection in each of the four final-state topologies. The observed WZ events are selected from the dataset collected during 2015 and 2016 that corresponds to an integrated luminosity of 13.3 fb^{-1}. The expected number of WZ events from Powheg+Pythia and the estimated number of background events from other processes are detailed. The signal WZ sample is normalised to NNLO cross section. The uncertainties quoted are only statistical [4].

Channel	eee	μee	$e\mu\mu$	$\mu\mu\mu$	All
Data	516	537	612	752	2417
Total Expected	504±7	588±5	552±6	671±4	2315±11
WZ	354.0±2.5	442.7±2.9	453.2±2.9	581.1±3.4	1831±6
ZZ	27.7±0.4	36.0±0.5	32.9±0.4	46.5±0.5	143.2±0.9
Misid. leptons	103±7	87±4	45±6	17.9±2.5	253±10
$t\bar{t}$+V	12.8±0.1	14.49±0.13	13.50±0.12	15.59±0.13	56.41±0.25
tZ	5.506±0.029	6.674±0.033	6.653±0.032	8.22±0.04	27.05±0.07
VVV	0.974±0.029	1.219±0.034	1.166±0.031	1.44±0.04	4.80±0.07

Table 3. Summary of the relative uncertainties in the measured fiducial cross section $\sigma^{\text{fid.}}_{W^{\pm}Z}$ for each channel and for their combination [4].

Channel	eee	μee	$e\mu\mu$	$\mu\mu\mu$	All
e energy scale	0.3	0.2	0.2	0.0	0.1
e id. efficiency	4.6	2.7	1.9	0.0	1.3
μ momentum scale	0.0	0.1	0.1	0.2	0.1
μ id. efficiency	0.0	1.3	2.6	3.7	2.6
E_T^{miss} and jets	0.5	0.4	0.8	0.9	0.8
Trigger	0.1	0.1	0.1	0.2	0.1
Pileup	0.5	1.2	1.4	1.1	1.1
Misid. leptons background	11.9	5.6	11.9	1.7	3.1
ZZ background	0.6	0.7	0.6	0.6	0.6
Other Irr. backgrounds	0.5	0.5	0.4	0.3	0.4
Uncorrelated	10.6	9.2	6.2	3.6	2.9
Total systematics	16.6	11.3	13.9	5.7	5.5
Luinosity	3.3	3.3	3.2	3.2	3.2
Statistics	6.2	5.3	5.3	4.1	2.7
Total	18.1	12.9	15.2	7.7	6.9

The SM NLO prediction from Powheg+Pythia is $53.4^{+1.6}_{-1.2}(PDF)^{+2.1}_{-1.6}(scale)fb$, which is obtained using the CT10 PDF set and by setting the dynamic QCD scales μ_R and μ_F to $m_{WZ}/2$.

Using the 3.2 fb^{-1} of the 2015 dataset, the combined fiducial cross-section was extrapolated to the total phase-space resulting:

$$\sigma^{tot.}_{W^{\pm}Z} = 50.6 \pm 2.6(stat.) \pm 2.0(sys.) \pm 0.9(th.) \pm 1.2(lumi.)pb \quad (2)$$

The SM NLO prediction calculated with Powheg+Pythia is $42.4 \pm 0.8(PDF) \pm 1.6(scale)pb$. A recent NNLO calculation [12] yields $48.2^{+1.1}_{-1.0}(scale)pb$, a result which is in better agreement with the measurement. Also, with the 2015 dataset the ratio of the $W^{\pm}Z$ production cross-section at the two centre-of-mass energies of 13 TeV over 8 TeV is also calculated and it is

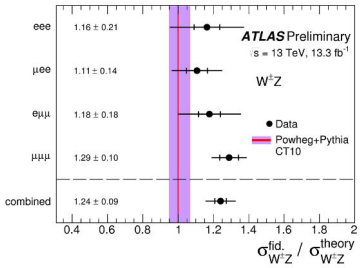

Figure 2. The integrated cross section in the fiducial phase space in each of the four channels and their combination. The inner and total error bars on data points represent the statistical and the total uncertainties, respectively. The measurement is compared to the prediction from Powheg+Pythia at NLO QCD [4].

$$\frac{\sigma^{fid.,13TeV}_{W^{\pm}Z}}{\sigma^{fid.,8TeV}_{W^{\pm}Z}} = 1.80 \pm 0.10(stat.) \pm 0.08(sys.) \pm 0.06(lumi.) \quad (3)$$

where all uncertainties are treated as uncorrelated and the result being in good agreement with the SM prediction from Powheg+Pythia of 1.78±0.03. Finally, the ratio of W^+Z to W^-Z is calculated

$$\frac{\sigma^{fid.}_{W^+Z\to\ell'\nu\ell\ell}}{\sigma^{fid.}_{W^-Z\to\ell'\nu\ell\ell}} = 1.39 \pm 0.14(stat.) \pm 0.03(sys.) \pm 0.06(lumi.) \quad (4)$$

The result is shown in Figure 3. It is dominated by the statistical uncertainty and it is compared to the SM prediction from Powheg+Pythia of $1.47^{+0.03}_{-0.06}$.

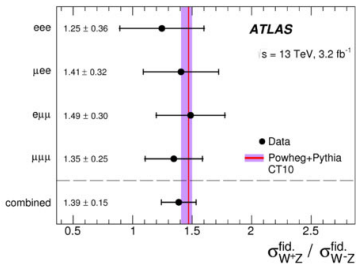

Figure 3. Measured ratios $\sigma^{fid.}_{W^+Z} / \sigma^{fid.}_{W^-Z}$ of W^+Z and W^-Z integrated cross sections in the fiducial phase space in each of the four channels and for their combination. The error bars on the data points represent the total uncertainties, which are dominated by the statistical uncertainties. The shaded violet band is the total uncertainty in this prediction [3].

4.2 Differential distributions

The differential cross-section as a function of the Z-boson p_T as well as the transverse mass of the WZ-system is presented in Figure 4. It is obtained by correcting for detector effects (such as finite resolution, limited acceptance and imperfect efficiency) as well as for QED FSR effects using a Bayesian iterative method [13, 14]. A response matrix, accounting for bin migration effects between the reconstructed and particle-level distributions, is obtained using Powheg+Pythia. The unfolded distributions are compared to the predictions from Powheg+Pythia and Sherpa, showing a very good description of the data.

Using the 2015 dataset the differential cross-section as a function of the jet multiplicity was also calculated and it is presented in Figure 5. The same iterative Bayesian method was used and the unfolded result is compared to the predictions from Powheg+Pythia and Sherpa. The shape of the measured cross section as a function of the jet multiplicity is described well by Sherpa, but it is reproduced poorly by Powheg+Pythia. The matrix-element calculation in the Sherpa prediction includes

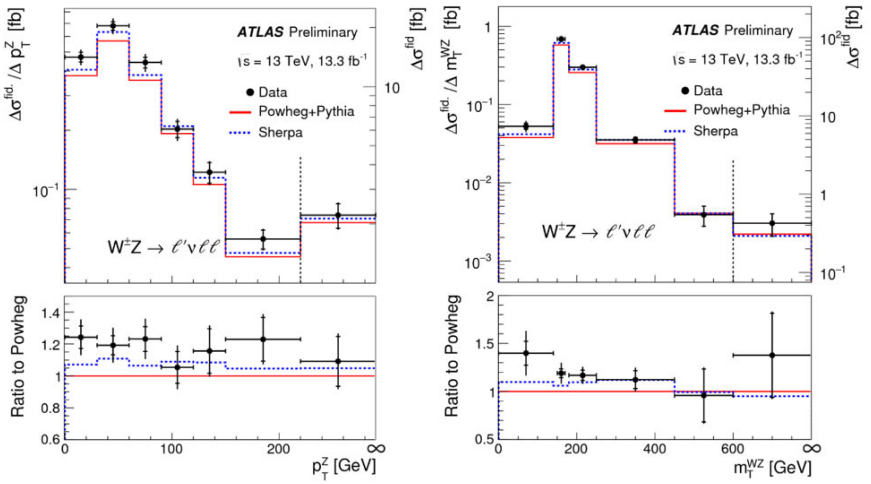

Figure 4. The measured $W^{\pm}Z$ differential cross section in the fiducial phase space as a function of the transverse momentum of the reconstructed Z-boson p_T (left) and the transverse mass variable m_T^{WZ} for the $W^{\pm}Z$ system (right). The inner and outer error bars on the data points represent the statistical and total uncertainties, respectively. The measurements are compared to the prediction from Powheg+Pythia (red line) and Sherpa (dashed blue line) at NLO QCD [4].

up to three jets at LO, while in the Powheg+Pythia prediction only the leading jet is included, and higher jet multiplicities are described by the parton shower models.

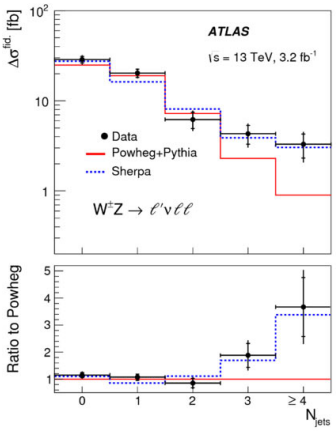

Figure 5. The measured $W^{\pm}Z$ differential cross section in the fiducial phase space as a function of the exclusive jet multiplicity of jets with $p_T > 25$ GeV. The inner and outer error bars on the data points represent the statistical and total uncertainties, respectively. The measurements are compared to the prediction from Powheg+Pythia (red line) and Sherpa (dashed blue line) [3].

4.3 Limits on anomalous triple gauge couplings

Two parametrisations are used to search for effects beyond the SM via aTGCs: one using an effective Lagrangian that describes the charged WWZ vertex, containing only terms that conserve the charge conjugation and parity [15, 16], where deviations from SM predictions are introduced as dimension-

less anomalous couplings $\Delta\kappa^Z, \Delta g_1^Z$ and λ^Z. In order to avoid violation of unitarity a form factor is introduced:

$$a(\hat{s}) = a(0)/(1 + \hat{s}/\Lambda_{co}^2)^2 \tag{5}$$

where $a(0)$ is the anomalous coupling value at low energy and Λ_{co} a cutoff scale related to the energy at which the effective field theory breaks down and new physics is expected to emerge.

In the second parametrisation, based on an effective field theory (EFT), the particle content of the SM is not changed and a linear combination of operators of mass dimension higher than four is added to the SM Lagrangian [17, 18].Three dimension-six C- and P-conserving operators that lead to aTGCs lead to the following new terms in the Lagrangian:

$$\begin{aligned} O_{WWW} &= \frac{c_{WWW}}{\Lambda_{NP}^2} Tr[W_{\mu\nu} W^{\nu\rho} W_\rho^\mu], \\ O_{WWW} &= \frac{c_W}{\Lambda_{NP}^2} (D_\mu \Phi)^\dagger W^{\mu\nu} (D_\nu \Phi), \\ O_B &= \frac{c_B}{\Lambda_{NP}^2} (D_\mu \Phi) B^{\mu\nu} (D_\nu \Phi) \end{aligned} \tag{6}$$

where $W_{ij}, W^{ij}, W_j^i (i = \mu, \nu, j = \nu, \rho)$ and $B^{\mu\nu}$ are built from the SM electroweak gauge boson fields, $D_i (i = \mu, \nu)$ are the covariant derivatives as introduced in the SM and Φ is the Higgs doublet field, as defined in [18]. Λ_{NP} represents the energy scale of new physics.

The two parametrisations may be considered equivalent since the anomalous couplings can be reinterpreted in terms of the EFT parametrisation. Confidence intervals are extracted from the transverse mass of the WZ system differential distribution at detector level, as shown in Figure 6. The presence of aTGCs would affect the integrated cross-section and is expected to increase the yields of the higher bins of the aforementioned distribution.

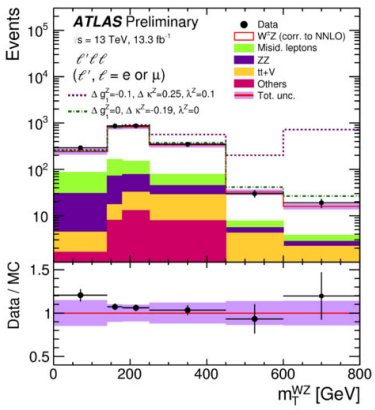

Figure 6. Distribution of m_T^{WZ} in the sum of all channels with the same binning as used for the calculation of aTGC confidence intervals. The points correspond to the data and the histograms to the expectations of the different SM processes. The shaded violet band its estimated total uncertainty [4].

The 95% confidence intervals are derived using the frequentists approach by using a profile likelihood that incorporates all systematic uncertainties as nuisance parameters. The cutoff scale is set to $\Lambda_{co} = \infty$ (no cutoff), as the current sensitivity is well within the unitarisation constraints. To improve the sensitivity the confidence intervals are also derived by combining the 8 TeV and 13 TeV datasets. Table 4 shows the expected and observed 95% confidence level intervals for $\Delta\kappa^Z, \Delta g_1^Z$ and λ^Z while Table 5 presents the interpretation of these intervals in terms of the EFT coefficients $c_{WWW}/\Lambda_{NP}^2, c_B/\Lambda_{NP}^2$ and c_W/Λ_{NP}^2. Finally, Figure 7 presents a comparison of the latest derived confidence intervals to those previously obtained using $W^\pm Z$ events gathered by ATLAS in $\sqrt{s} = 7$ TeV and $\sqrt{s} = 8$ TeV.

Table 4. Expected and observed one-dimensional 95% CL intervals for the anomalous coupling parameters using $\Lambda_{co} = \infty$ [4].

Dataset	Coupling	Expected	Observed
13 TeV	Δg_1^Z	[-0.017; 0.032]	[-0.016; 0.036]
	$\Delta\kappa_1^Z$	[-0.18; 0.24]	[-0.15; 0.26]
	λ^Z	[-0.015; 0.014]	[-0.016; 0.015]
8 and 13 TeV	Δg_1^Z	[-0.014; 0.029]	[-0.015; 0.030]
	$\Delta\kappa_1^Z$	[-0.15; 0.21]	[-0.13; 0.24]
	λ^Z	[-0.013; 0.012]	[-0.014; 0.013]

Table 5. Expected and observed one-dimensional intervals at 95% CL for the EFT parameters extracted from 13 TeV WZ measurement standalone and from combined 8 and 13 TeV datasets [4].

Dataset	Coupling	Expected $[TeV^{-2}]$	Observed $[TeV^{-2}]$
13 TeV	c_W/Λ^2_{NP}	[-4.1; 7.6]	[-3.8; 8.6]
	c_B/Λ^2_{NP}	[-261; 193]	[-280; 163]
	c_{WWW}/Λ^2_{NP}	[-3.6; 3.4]	[-3.9; 3.7]
8 and 13 TeV	c_W/Λ^2_{NP}	[-3.4; 6.9]	[-3.6; 7.3]
	c_B/Λ^2_{NP}	[-221; 166]	[-253; 136]
	c_{WWW}/Λ^2_{NP}	[-3.2; 3.0]	[-3.3; 3.2]

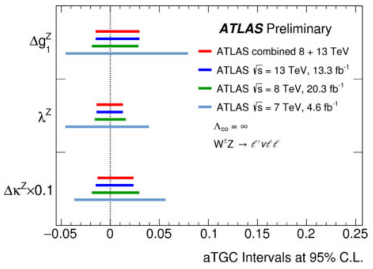

Figure 7. Comparison of one-dimensional intervals at 95% CL for the anomalous coupling parameters using a cutoff scale of $\Lambda_{co} = \infty$ and obtained from the analysis of $W^{\pm}Z$ events at different centre-of-mass energies by the ATLAS experiment. The confidence intervals for $\Delta\kappa^Z$ parameter are scaled down by a factor of 10 [4].

5 Conclusions

Measurements of the $W^{\pm}Z$ production cross-section, integrated and differentially with respect to various observables have been presented. The data analysed were collected by the ATLAS detector in LHC during 2015 and 2016 and correspond to a total integrated luminosity of 13.3 fb^{-1}. Purely leptonic decay modes to electrons and muons were considered; the measured cross-sections are well described by SM predictions.

Using the reconstructed distribution of the $W^{\pm}Z$ system at detector level a search for the presence of aTGCs was performed and confidence intervals for $\Delta\kappa^Z, \Delta g_1^Z$ and λ^Z were derived, providing the most stringent confidence intervals for WWZ anomalous couplings to date. The results were also interpreted as confidence intervals for the coefficients of the $c_{WWW}/\Lambda^2_{NP}, c_B/\Lambda^2_{NP}$ and c_W/Λ^2_{NP} EFT parametrisation.

References

[1] ATLAS Collaboration, JINST 3, S08003 (2008)
[2] ATLAS Collaboration, Phys.Rev. D93 no.9, 092004, (2016)
[3] ATLAS Collaboration, Phys.Lett. B 762, 1-22 (2016)
[4] ATLAS Collaboration, ATLAS-CONF-2016-043, (2016)
[5] ATLAS Collaboration, JHEP 04 (2015)
[6] S. Frixione, P. Nason, and C. Oleari, JHEP 0711 (2007)
[7] T. Sjostrand, S. Mrenna, and P. Z. Skands, Comput. Phys. Commun. 178 (2008)
[8] ATLAS Collaboration, JHEP 1409 (2014)
[9] A. Glazov, AIP Conf. Proc. 792 (2005)
[10] H1 Collaboration, Eur. Phys. J. C 63 (2009) 625
[11] H1 Collaboration, ZEUS Collaboration, J. High Energy Phys. 1001 (2010)
[12] M. Grazzini, S. Kallweit, D. Rathlev, M. Wiesemann, $W^{\pm}Z$ production at hadron colliders in NNLO QCD, 2016, arXiv:1604.08576 [hep-ph]
[13] G. D'Agostini, Nucl. Instrum. Meth. A 362 (1995)
[14] T. Adye, Unfolding algorithms and tests using RooUnfold, Proceedings of the PHYSTAT 2011 Workshop, CERN, Geneva, Switzerland (2011) 313, arXiv: 1105.1160 [physics.data-an].
[15] K. Hagiwara et al., Nucl. Phys. B 282 (1987)
[16] J. Ellison and J. Wudka, Ann. Rev. Nucl. Part. Sci. 48 (1998)
[17] W. Buchmuller and D. Wyler, Nucl. Phys. B 268 (1986)
[18] C. Degrande et al., Annals Phys. 335, (2013)